Thermal Conductivity of Fluid He^3 and He^4 at Temperatures between 1.5 and 4.0° K and for Pressures up to 34 atm*†

Jerry F. Kerrisk and William E. Keller
Los Alamos Scientific Laboratory, University of California, Los Alamos, New Mexico 87544
(Received 5 August 1968)

Measurements of the thermal-conductivity coefficient κ are reported for liquid He^4 I between 1.77 and 3.95° K, for fluid He^3 between 1.5 and 3.95° K, both at pressures up to 34 atm, and for gaseous He^3 and He^4 between 1.5 and 3.95° K at ~10 Torr. Special attention is given the liquid-vapor critical region of He^3 and the λ-transition line of He^4. Corrections for effects of thermal boundary resistance and convection are discussed for the fixed-separation parallel-plate apparatus used for these experiments. Taking into account these corrections, the over-all accuracy of the data is considered to be better than ± 3%, though the precision is better than ± 1%. Away from the singular regions $(\partial\kappa/\partial T)_P$ is anomalously positive and increases with pressure for both He^3 and He^4. Isobars of κ for He^4 I pass through shallow minima and then rise sharply as the λ line is approached from higher temperature. Isotherms of κ for He^3 in the neighborhood of the critical point display distinct cusps. Scaling laws predict that near the λ temperature T_λ the coefficient κ should be proportional to $(T-T_\lambda)^{-1/3}$, and near the critical temperature T_c it should be proportional to $|T-T_c|^{-2/3}$; other theories predict κ to be proportional to $|T-T_c|^{-1/2}$ near T_c. The experimental data are found to agree qualitatively, but not quantitatively, with these predictions.

We present here the method and results of experiments which measure the coefficient of thermal conductivity κ of fluids He^3 and He^4 at low temperature and at pressures up to 34 atm. The regions of the pressure-temperature plane covered by this research as well as by previous work are shown schematically in Fig. 1 (He^3) and Fig. 2 (He^4). In addition we have obtained κ for the vapor at ~10 Torr for both isotopes. Results for He^4 are confined to the liquid He I region, where the liquid behaves relatively normally, since the apparatus was not designed to measure the unusually large heat conductivity found in superfluid He II.

Motivation for the present work comes from several sources. Firstly, previously reported[1–4] values of κ for liquid He^4 I near saturation conditions lack consistency and generally display considerable scatter; the situation is similar for the earlier liquid He^3 work[3,4] above 1.2° K and at low pressure. Consequently, a principal aim of this research is to provide accurate, smooth values

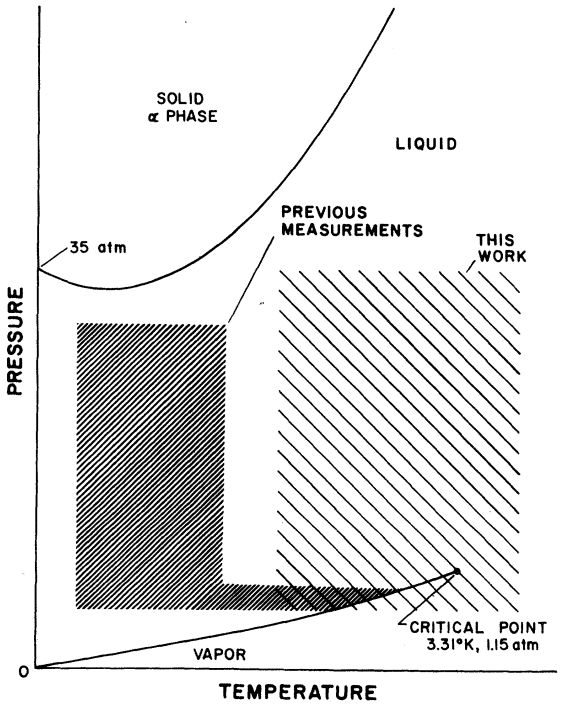

FIG. 1. Schematic P–T phase diagram for He^3 showing regions covered by the present and previous thermal-conductivity investigations.

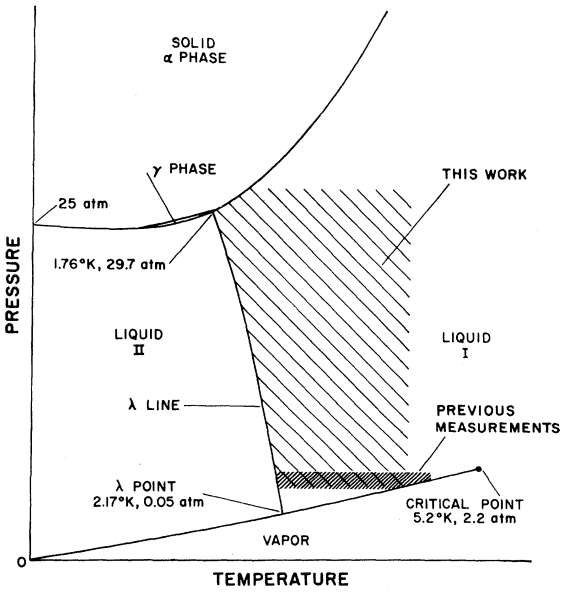

FIG. 2. Schematic P–T phase diagram for He^4 showing regions covered by the present and previous thermal-conductivity investigations.

of κ for He^3 and He^4 over a significant range of P and T. Secondly, the existing thermal-conductivity data on the quantum fluids He^3 and He^4 has established that well above the degeneration temperature the coefficient $(\partial\kappa/\partial T)_P$ for small P is anomalously positive. Further exploration of the $\kappa(T, P)$ behavior appears warranted. Finally, we note from Figs. 1 and 2 that the range of the present investigation includes the liquid-vapor critical point of He^3 and extends along the λ line of He^4. Very little is known about the transport properties of ordinary fluids in the vicinity of thermodynamic singular points; even more obscure is the role played by quantum effects in these instances. In addition the entire relationship between the λ transition and general critical phenomena requires clarification, so that experimental transport data close to the singularities are of great current interest.

I. APPARATUS AND EXPERIMENTAL METHOD

For a steady heat flux $\vec{q}$ the coefficient of thermal conductivity of a medium is defined through Fourier's law for diffusive heat flow as

$$\vec{q} = -\kappa \nabla T , \qquad (1)$$

where ∇T is the temperature gradient in the direction of $\vec{q}$ in the specimen. If κ is a weak function of temperature, or in the limit of vanishing temperature difference ΔT across the medium, ∇T may be well approximated by $\Delta T/l$, the quantity l being the distance separating the points at which ΔT is determined (we consider linear geometries and assume the temperature gradient is in one direction only). It is immediately obvious that in an experiment performed to obtain reliable values of $\kappa(T, P)$ for fluid He one must strive for high accuracy in measurements of T, ∇T, $\vec{q}$, P, and l. Furthermore, in the actual situation there are thermal effects in addition to those described by Eq. (1), including: heat conduction through paths other than the fluid medium in question (container walls, electrical leads, etc.), convective heat transfer through the fluid medium, radiative heat transfer, and the thermal-boundary resistance between the walls of the container and the medium. These effects must be either eliminated or accurately accounted for.

A thermal-conductivity cell designed to satisfy the above requirements is shown schematically in Fig. 3. The type of measurement used here is an example of the so-called "flat plate" method. The sample of fluid He is contained in the volume between two comparatively massive copper plates and bounded by a stainless-steel ring (i.d. = 2.54 cm; wall thickness at fluid layer = 0.025 cm). A narrow inlet (d = 0.036 cm) at the center of the bottom plate permits introduction of He into the sample space without significantly altering the critical cell geometry. Both the He layer and the upper plate are enclosed in the evacuated inner can, while the bottom plate is immersed in a thermostated bath of He^4. Heat delivered to the top plate produces across the He layer a temperature difference which is detected by thermometers embedded in the copper plates. Electrical leads (No. 40 Copper) for the hot-side thermometer and the heater are taken out of the vacuum space into the He^4 bath via glass-metal pin seals. An outer thick-walled copper can surrounds the cell assembly for the purpose of minimizing thermal gradients in the vicinity of the cell when He I is the thermostatic fluid. (This can has several holes to allow free passage of the He^4 bath.)

A. Temperature Measurements

Both cell thermometers are Allen-Bradley $\frac{1}{4}$ W carbon composition resistors (nominal resistance 140 Ω). Resistances were measured with a dc Wheatstone bridge using a constant voltage (0.020 V) such that the heat dissipated in each thermometer was always less than 10^{-7} W. Conversion of resistance to temperature on the 1958 He^4 scale[5] was accomplished via measurements of the bath vapor pressure P_{sat} as read on either a di-n-butyl sebecate manometer ($P_{sat} < 40$ Torr) or a Hg manometer ($P_{sat} > 40$ Torr). The bridge is designed to measure either the resistance of each thermometer separately or the difference in resistance between the two. Although each resistor is ~1.2 cm from the nearest He-Cu boundary, because the thermal conductivity of copper in the temperature range of interest is of the order of 10^4 times that of He, less than 0.3% of the total measured ΔT between thermometers occurs in the copper plates. For making measurements of κ, values of ΔT were chosen such that the estimated error in the smallest ΔT imposed was less than 1%. Exceptions to this rule occurred

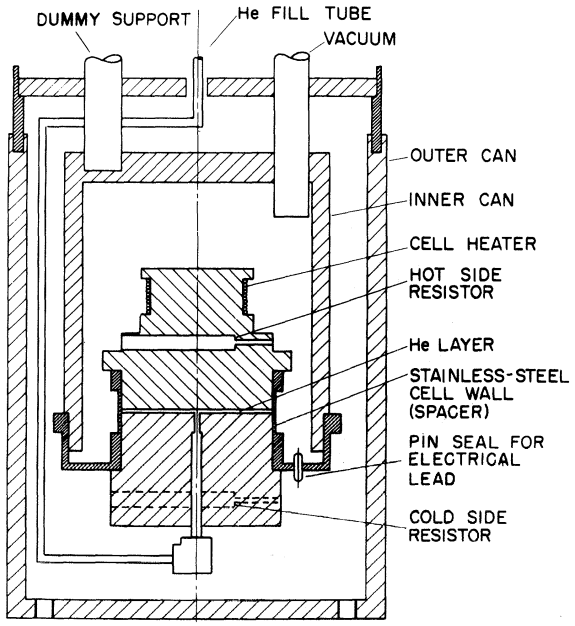

FIG. 3. Thermal-conductivity cell.

for some measurements very close to the He^4 λ-line, where in some cases ΔT was less than 10^{-4} °K with an accompanying error as high as 10%.

Two different electronic bath-temperature controllers were used to obtain steady reference temperatures T_0: one[6] when the bath was He II, the other[7] when it was He I. In both cases during a given thermal-conductivity measurement (~20 min) T_0 varied less than 10^{-4} °K as indicated by bath vapor-pressure monitorings.

B. Cell Heater

Power for the cell heater (100 Ω of Manganin wire wound around the top of the upper copper plate) is supplied by a 2 V shielded battery and controlled by a 50 kΩ variable resistance in series with the heater. The heater current (I) was determined by measuring the potential drop across a 100.00-Ω standard resistor; and potential (V) measurements were made at the point where the heater leads exited from the inner can (the resistance of the current leads from this point to the heater was always less than 10^{-3} Ω, giving negligible heating compared with the heater proper). The estimated error in the power measurement ($Q=IV=A\tilde{q}$, where A is the plate area) is ±0.1%.

C. Pressure Measurements

Pressures of the sample He were determined with a Texas Instruments fused-quartz Bourdon-tube pressure gauge situated outside the cryostat. Capsules for two useful pressure ranges, 0 to 34 atm, and 0 to 7 atm, are available: the former was used for most pressure measurements, the latter for some additional points near the He^4 λ transition and for all data near the He^3 critical point. Before use, both capsules were calibrated over their entire range with a Ruska Instrument Corp. Model-2460 dead-weight gauge. The sensitivity of the 0- to 34-atm capsule is ±0.001 atm and the estimated accuracy is ±0.003 atm; the corresponding figures for the 0- to 7-atm capsule are ±0.0001 and ±0.001 atm.

D. Plate Separation

We have chosen to use a fixed plate-separation distance l rather than variable l as used in some of the earlier He I work.[1] The present scheme has the advantages of allowing l to be easily and accurately measured and of providing a single, stable geometry for the entire P and T ranges covered for both isotopes. It has the disadvantage of complicating the estimation of thermal boundary resistance since this is usually accomplished by changing l (see below). In order to overcome this difficulty, after the complete sets of measurements were taken with an initial value of $l=l_1$, the separation distance was reduced to a new value, l_2, by removing the top copper plate and remachining the top of the stainless-steel cell wall (spacer).

In assembly of the cell, the spacer was first silver soldered to the bottom copper plate; the inside surfaces were then machined (to square the corners and remove excess solder), cleaned and polished; and finally, the clean top plate was carefully soft soldered to the spacer while an oxygen-free atmosphere was maintained in the sample space. Radiographic inspection of the completed cell gave assurance that no foreign matter was lodged between the plates and especially that no "blobs" of soft solder had formed in the sample space.

Values of l were derived from thickness measurements of the separate plates and of the assembled cell. In each case micrometer readings accurate to ±0.00013 cm were taken at eight equally spaced locations around the plates. The results were $l_1=0.0820$ cm and $l_2=0.0602$ cm. From the spread in the readings we estimate that each of these represents the average spacing to better than 1%. Calculations of the change of l with pressure indicate that at 34 atm, $\Delta l/l<0.05\%$. A correction was made to the plate separation and diameter to account for thermal contraction between room temperature and liquid He temperature.

E. Experimental Procedure

In applying Eq. (1) to the present apparatus we note that there are three parallel paths for diffusive heat flow from the upper heated plate to the thermal sink: across the He layer, through the electrical leads, and through the stainless-steel cell wall. Consequently, a set of measurements of Q and ΔT gives not κ for He, but instead some other coefficient, which we call κ_T, representing the over-all thermal conductivity. Now, Lazarus[8] has demonstrated that for the type of geometry in question and for a given ΔT the total heat flow through a set of parallel paths, each of which may be characterized by a separate $\kappa(T)$, is independent of whether the paths are in contact or are insulated from one another. We are then justified in decomposing κ_T as

$$\kappa_T=\kappa+\kappa_c\,, \tag{2}$$

where κ_c represents the nonhelium paths. Therefore, we may obtain κ for He from measurements of both κ_T and κ_c, the latter being just the effective thermal conductivity of the empty cell. In practice, for Eq. (2) to be valid, it is necessary that the cross section of the cell wall be at the same temperature as the upper (hot) plate at the point of contact between wall and plate: and similarly for lower (cold) plate. That this was indeed so was checked by numerical calculation of the temperature distribution for the ranges of ΔT's used in the experiments.

Prior to the He runs, the empty cell was calibrated over the temperature range to be investigated. For the cell with separation l_1 the quantity κ_c was found to vary nearly linearly from 0.28×10^{-4} W/cm °K at 1.5°K to 0.90×10^{-4} W/cm °K at 4.0°K. From the data subsequently obtained for He^3 at 4 atm, for example, κ_c/κ_T is about 0.2 and 0.33 at the respective temperatures just

mentioned. Incidentally, the contribution to κ_c from the copper leads is small (~1%) so that κ_{SS}, the conductivity of the stainless-steel spacer, can be calculated from κ_c. The results of these determinations of κ_{SS} agree well with those found in the literature.

As a rule, a given run consisted of measurements of κ made at constant T_0 and at various pressures. Consequently, the cell was filled with He initially to the highest pressure, with subsequent points on an isotherm obtained after bleeding gas from the system. On various isotherms, points were taken at nearly the same pressures so that isobars could be easily constructed. He^4 gas was taken directly from a high-pressure commercial cylinder and purified through a liquid-N_2–cooled charcoal trap before being admitted to the sample chamber. High pressures for the He^3 sample (99.62% He^3, 0.38% He^4) were obtained by first condensing the gas in a bomb and then warming up the bomb.

Each measurement of κ at a given T_0 and P was obtained from a series of Q-versus-ΔT determinations. Where κ is a weak function of T, three such determinations were deemed sufficient, with ΔT ranging usually between 1×10^{-3} and 8×10^{-3} °K. However, near the He^3 critical point and the He^4 λ line, κ varies rapidly with T; here as many as eight Q-ΔT measurements (with ΔT as low as 4×10^{-5} °K) were made for a given T_0 and P.

II. METHOD OF DATA ANALYSIS

Under the assumptions that Q is not a function of T, that κ is not an explicit function of x, that ∇T is only in the x direction, and that the heat flux is uniformly distributed over A, Eq. (1) may be separated and integrated to give

$$\int_0^l Q\,dx = -A\int_{T_0+\Delta T}^{T_0}\kappa\,dT\,, \tag{3}$$

or

$$Q = (A/l)\int_{T_0}^{T_0+\Delta T}\kappa\,dT\,. \tag{4}$$

In general, κ is a function of T; and we may expand $\kappa(T)$ in a Taylor series about T_0 to give

$$\kappa(T) = \kappa(T_0) + \frac{d\kappa}{dT}\Big|_{T_0}(T-T_0) + \frac{d^2\kappa}{dT^2}\Big|_{T_0}\frac{(T-T_0)^2}{2} + \cdots\,. \tag{5}$$

Substituting Eq. (5) into Eq. (4) and evaluating the integral term by term, we find

$$Q(T_0,\Delta T) = \frac{A}{l}\left(\kappa(T_0)\Delta T + \frac{1}{2}\frac{d\kappa}{dT}\Big|_{T_0}(\Delta T)^2 + \frac{1}{6}\frac{d^2\kappa}{dT^2}\Big|_{T_0}(\Delta T)^3 + \cdots\right)\,. \tag{6}$$

When κ is a weak function of T and ΔT is small, only the first term in Eq. (6) is important. We then have the familiar expression

$$\kappa(T_0) = (l/A)\,Q(T_0,\Delta T)/\Delta T\,. \tag{7}$$

Except near the He^3 critical point and the He^4 λ line, plots of Q versus ΔT for constant T_0 were straight lines indicating the validity of the approximation of Eq. (7). In this way $\kappa_T(T_0)$ for the full cell was obtained, with $\kappa(T_0)$ subsequently derived by subtracting off κ_c determined previously for the empty cell.

When systematic curvature appeared in the Q-versus-ΔT plots additional terms of Eq. (6) were included. For He^3 near the critical point the quadratic approximation served well; but for He^4 in the vicinity of the λ line it was necessary to include the term cubic in ΔT. A nonlinear relation between Q and ΔT does not necessarily mean that κ varies strongly with T in the ΔT interval investigated. For if convection is important, this will introduce curvature even though κ is effectively constant; and then the physical meaning of such parameters as $d\kappa/dT$ must be ascertained by independent estimates of the contribution of convection (see below).

The experimental Q-versus-ΔT data have been fitted by Eq. (6) using a method of least squares due to Deming.[9] Whereas in the usual least-squares scheme all the error is assumed to reside in the dependent variable (Q in the present case), Deming's method allows the least-squares adjustment of data for which both the dependent and independent variables may contain errors. Our estimated error in Q is ±0.1% and that in ΔT at least ±1%.

III. THE EFFECTS ON κ DUE TO CONVECTION AND BOUNDARY RESISTANCE

A. Convection

In addition to diffusive heat flow across the sample fluid, radiative and convective heat transfer may contribute to the over-all observed κ. The former is completely negligible for the low temperatures used in these experiments; but the effects of convection can be particularly troublesome, especially for data taken in the vicinity of the phase singularities. Near the He^3 critical point and in the vicinity of the He^4 λ line the observed thermal conductivity increases, as does the tendency for convection to occur. Hence it is necessary to determine whether this increase in κ is real or arises from convection. The two regions will be considered separately.

Near the He^3 critical point our initial discussion is based on the analysis by Michels and Sengers[10] of convection in a horizontal parallel-plate cell due to small deviations of the plates from the horizontal. Even though the fluid has a positive isobaric thermal-expansion coefficient and is heated from above, convection can occur if the fluid layer is tilted. Michels and Sengers[10] showed that the apparent increase in the thermal-conduc-

tivity coefficient due to convection, $\delta\kappa$, could be related to the true coefficient κ by the relation

$$\delta\kappa/\kappa \leq (l/D) N_R \sin\varphi/180\pi , \quad (8)$$

where $N_R = g\alpha_P \rho^2 C_P \Delta T l^3/\kappa\eta$ (9)

is the Rayleigh number (dimensionless). In these relations D is the plate diameter, φ the angle between the plates and horizontal, g the acceleration due to gravity, α_P the isobaric expansion coefficient, ρ the fluid density, C_P the isobaric heat capacity, and η the coefficient of viscosity of the fluid. In the design and operation of a thermal-conductivity apparatus the experimenter may control φ, l/D, and ΔT, all of which should be minimized to eliminate convection effects. On the other hand, both α_P and C_P become exceedingly large near the critical point; and on the critical isochore in the limit as $T \to T_c$, the critical temperature, convection cannot be avoided.

In the present work, from the cell geometry and alignment, $\delta\kappa/\kappa$ was found to be $\sim 3\times10^{-8} N_R$; and an evaluation of N_R for He^3 showed that the contribution to κ from convection should not become significant (>1%) except for $T - T_c < 0.2°K$. Since much of the data taken near the He^3 critical point was along isotherms closer than this limit, an additional examination is required.

If Eq. (6) is used to calculate κ, the value obtained is at T_0, i.e., in the limit of $\Delta T \to 0$. Since the additional contribution from convection (when it is small) is proportional to ΔT, as noted in Eqs. (8) and (9), $\kappa(T_0)$ will not be influenced by convection as long as Eq. (6) is valid. The contribution from convection will be included in the coefficients $d\kappa/dT$, $d^2\kappa/dT^2$, etc., along with the true temperature variation of κ. Because convection can only add to the total heat transfer, the convective contribution to these coefficients will be positive. The validity of Eq. (6) depends on the size of the higher-order terms. Except for five isotherms in the critical region, Q was a linear function of ΔT, indicating that away from T_c the true κ depends weakly on T and that convection was absent. In the critical region, only terms through the quadratic in ΔT were used in Eq. (6). The maximum contribution of the quadratic term (including both convection and the temperature variation of κ) was 20% of the total Q. An estimate of the portion of the quadratic term due to convection indicates that it was less than half, giving a maximum of 10% increase in the heat transfer due to convection. We feel that the values of κ reported for He^3 in the critical region do not include any significant contribution from convection.

For He^4 near the λ line we have a different problem. Although the singularities in the thermodynamic quantities are not nearly so strong as in the case of the He^3 critical point, there is a region of the He I P-T phase diagram (bounded by the λ line and the dashed curve in Fig. 2) in which the expansion coefficient α_P is negative. Thus for the apparatus shown in Fig. 3, when heat is supplied to the top plate the liquid near the top of the cell should be denser than that near the bottom. In a gravitational field we then have an inherent driving force for convection.

Initial results obtained with the cell configuration of Fig. 3 gave strong indications that the rise in κ_{obs} near the λ line was completely independent of convection (for isotherms just below T_λ, the rise in κ_{obs} begins in a region when α_P is clearly positive). However, in order to determine unambiguously whether convection played a role in the results, additional experiments were performed. After all the measurements on both He^3 and He^4 were taken with the original geometry, the inner can was inverted, leaving the cell intact but permitting the heat current to flow upward through the fluid layer. Results with this inverted configuration for an isotherm at 2.10°K and for pressures as close as 10^{-2} atm to P_λ reproduced within 1% the original data taken using the normal configuration. Thus the effect of a negative α_P was shown to be negligible. In addition, a theoretical analysis[11] of a fluid with a negative α_P and heated from above predicts that contributions by convection should be significant only for values of $(T_0 - T_\lambda)$ smaller than used in these experiments.

B. Boundary Resistance

As the result of a heat flow Q across a solid-liquid or a solid-gas interface, a temperature drop ΔT_B generally occurs at the boundary. In the present situation the observed temperature difference, ΔT_{obs} should then be larger than the ΔT across the He layer alone; and the thermal-conductivity calculated on this basis using Eq. (7) would be lower than the true κ. In order to correct for this effect we may associate ΔT_B with a boundary resistance R_B which is in series with the thermal resistance of the fluid layer, $R = (\kappa A/l)^{-1}$. Thus the total resistance to heat transfer (in the absence of convection) is $R_T = R_B + R$. We then have

$$Q = \Delta T_{obs}/R_T = \Delta T_{obs}/[R_B + (\kappa A/l)^{-1}] , \quad (10)$$

which on rearrangement becomes

$$Ql/A\Delta T_{obs} = \kappa/(1 + \kappa R_B A/l) . \quad (11)$$

Because the left-hand side of Eq. (11) is just the observed thermal conductivity κ_{obs}, the ratio of κ_{obs} to the true conductivity is

$$\kappa_{obs}/\kappa = 1/(1 + \kappa R_B A/l) . \quad (12)$$

For $R_B = 0$, $\kappa_{obs} = \kappa$, and for $R_B \neq 0$, $\kappa_{obs} < \kappa$.

The two unknowns in Eq. (12), i.e., κ and R_B, can be determined from experiments with two different cell geometries, all other factors being fixed. With the present apparatus it was most convenient to vary l as discussed in Sec. I (D). By differentiating κ_{obs} in Eq. (12) with respect

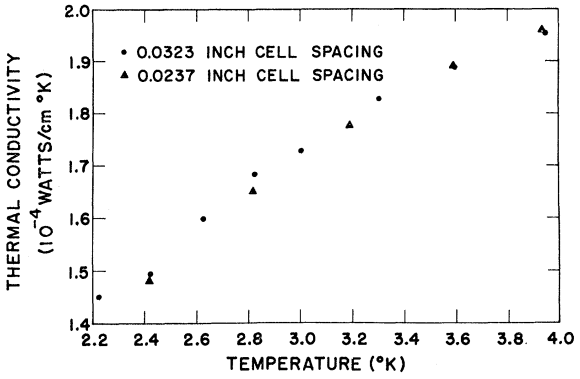

FIG. 4. Thermal conductivity of liquid He^4 as a function of temperature for two different cell spacings ($P=1$ atm).

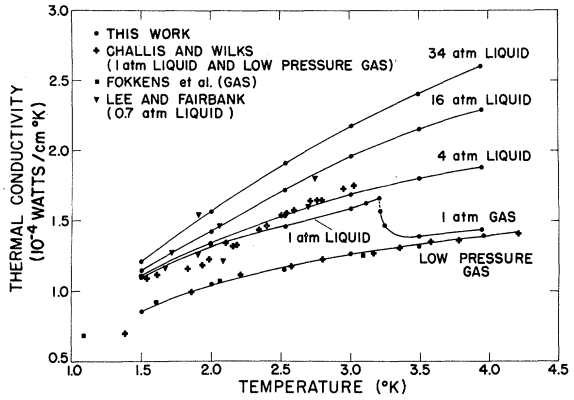

FIG. 5. Coefficient of thermal conductivity of fluid He^3 as a function of temperature at several pressures; present results compared with earlier data at low pressure.

to l we learn that a decrease in l should decrease κ_{obs} if the boundary resistance is significant. However, as shown in Fig. 4 an approximately 25% reduction in l appears to make no change in κ_{obs} to within experimental error. The uncertainty in the agreement between the two sets of data is ~ 1%, which places an upper limit of 3% on the possible error in κ due to boundary resistance. This constitutes the principal source of error in the absolute accuracy of the data reported here.

IV. RESULTS AND DISCUSSION

A. Gaseous Helium

Table I lists the results found for κ at several temperatures for low-pressure He^3 and He^4 gas. Each value of κ is an average of three or four Q-ΔT measurements. These κ data are also graphed in Figs. 5 and 6, where they are compared with earlier work. The agreement between the present results and those of Challis and Wilks[3] and of Fokkens *et al.*[12] for both isotopes is indeed gratifying.

The temperature dependence of κ for gaseous helium is quite normal; the relative magnitude of κ for He^3 and He^4 at a given temperature is anomalous. Classically we expect κ to be proportional to $m^{-1/2}$, where m is the atomic mass; but we see, for example, that at 3°K,

$$\kappa(He^3)/\kappa(He^4) = 2.11$$

rather than $(\frac{4}{3})^{1/2} = 1.15$. The differences are accountable in terms of quantum effects for the

TABLE I. Thermal conductivity of gaseous He. Numbers in parenthesis indicate number of Q-ΔT points used in obtaining the average value of κ.

He^4, $P\sim 10$ Torr		He^3, $P\sim 15$ Torr	
T(°K)	$10^5\kappa$(W/cm °K)	T(°K)	$10^5\kappa$(W/cm °K)
2.080	3.815 (3)	1.500	8.568 (4)
2.231	4.312 (4)	1.500	8.551 (3)
2.578	4.950 (3)	1.999	10.49 (4)
2.695	5.329 (3)	2.526	11.50 (4)
2.999	5.928 (4)	3.004	12.64 (4)
3.299	6.673 (3)	3.495	13.17 (4)
3.594	7.235 (3)	3.955	13.97 (4)
3.948	7.967 (3)		

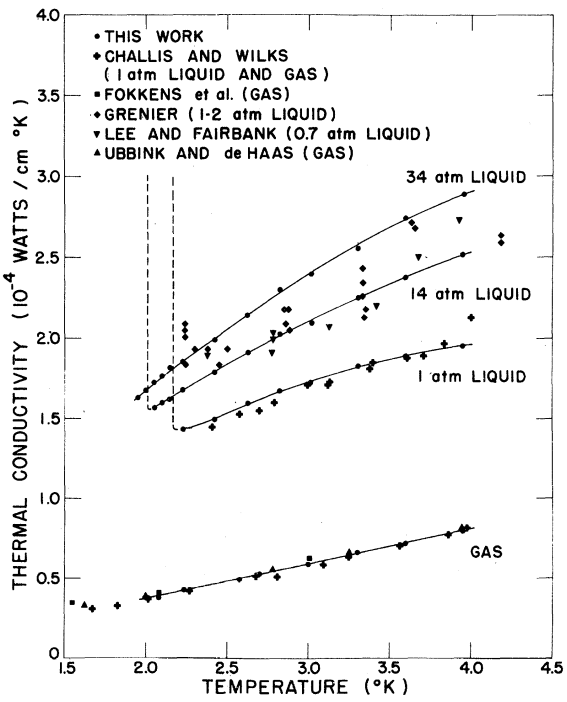

FIG. 6. Coefficient of thermal conductivity of fluid He^4 as a function of temperature at several pressures; present results compared with earlier data at low pressure.

He systems; and quantum calculations[12] using reasonable He-He intermolecular potentials are in agreement with the experimental observations.

B. Liquid He^4 and Fluid He^3 Well Away from Singular Regions

For liquid He^4 I some 224 values of κ have been measured on 21 isotherms covering the range indicated in Fig. 2. Similarly for fluid He^3, 132 determinations of κ were made along 26 isotherms. All of the raw data and derived values of κ are listed in Kerrisk's thesis.[13] Here we give samples of the results in graphical form, plus a tabulation for one isotherm for He^4 illustrative of the data obtained (Table II). Away from the respective thermodynamic singular points, the results for He^3 and He^4 are sufficiently similar that they may be considered together. Later we discuss separately the λ-transition region in He^4 and the critical point of He^3.

Figures 5 and 6 show κ as a function of T for the two liquids at several pressures. The solid lines through the solid circles represent the present measurements, while the remaining data for the liquids are for $P \sim 1$ atm as obtained by other workers. Clearly, of the earlier data the only values of κ quantitatively consistent with ours are those of Challis and Wilks.[3] These authors used a cell similar to ours but took no account of the boundary resistance, which, in view of the findings here, probably was not an important correction. The figures confirm that for both isotopes away from the critical regions, $(\partial\kappa/\partial T)_P$ is anomalously positive [in comparison with $(\partial\kappa/\partial T)_P$ for simple classical fluids such as Ar, N_2, CO_2, NH_3, CH_4, etc.] and, in addition, indicate that with increasing pressure this coefficient becomes larger. No theoretical explanation for this behavior is yet available.

TABLE II. Thermal-conductivity coefficients for He^4 as a function of pressure for $T = 2.100°K$, determined by extrapolating Q versus ΔT data to $\Delta T = 0$. In the last column N gives the number of experimental Q-ΔT points used to determine κ.

T(°K)	P(atm)	$10^4\kappa$(W/cm °K)	N
2.0996	33.991	1.773	3
2.0997	31.997	1.782	3
2.0997	29.919	1.768	4
2.0998	28.009	1 745	3
2.0999	26.025	1.724	3
2.0999	24.036	1.702	3
2.0999	21.963	1.693	3
2.0999	19.980	1.672	3
2.1000	18.001	1.656	3
2.1000	16.016	1.630	3
2.1000	14.031	1.607	3
2.0997	11.977	1.576	3
2.0997	10.005	1.566	3
2.0997	8.973	1.590	3
2.0998	7.947	1.680	3
2.0999	7.472	1.794	4
2.0999	7.005	2.669	4
2.1000	6.927	3.169	4
2:1000	6.864	7.256	4
2.1000	6.853	9.205	4
2.1000	$P_\lambda = 6.852$		

TABLE III. Parameters for Eq. (13) for κ in units of W/cm °K and pressure in units of dyn/cm^2.

Parameter	Liquid He^4	Liquid He^3
F_0	-1.4642×10^{-5}	1.8501×10^{-5}
F_1	8.8025×10^{-5}	6.5501×10^{-5}
F_2	9.1386×10^{-13}	0[a]
F_3	-8.7000×10^{-6}	-6.2602×10^{-6}
F_4	-4.1701×10^{-20}	-2.2759×10^{-20}
F_5	8.3023×10^{-13}	8.2703×10^{-13}

[a]For He^3, allowing F_2 to be nonzero gives no better a fit than when F_2 is fixed at zero.

Results for κ of both fluids in phase regions not affected by thermodynamic abnormalities have been fitted to polynomials of the form

$$\kappa(T,P) = F_0 + F_1 T + F_2 P + F_3 T^2 + F_4 P^2 + F_5 PT. \quad (13)$$

Parameters appropriate for He^3 and He^4 are listed in Table III. For the 75 observations of κ for He^4 so fitted, the maximum deviation is 3%; for 37 He^3 points the maximum deviation is 2.8%. Hence Eq. (13) is believed to be a reliable interpolation formula; but since it does not represent the increases of κ near $T_\lambda(P)$ or T_c, it should not be extrapolated into these regions.

At temperatures below 1°K, Anderson *et al.*[14] have measured κ for He^3 with results schematically shown in Fig. 7. In contrast with the higher-temperature data where $(\partial\kappa/\partial P_T) > 0$, below 1°K $(\partial\kappa/\partial P)_T < 0$; also for each pressure the curve passes through a minimum and, at the lowest temperatures, rises in a manner believed to be a precursor of Fermi liquid behavior,[15] i.e., $\kappa \propto T^{-1}$. The crossing of the isobars has not yet

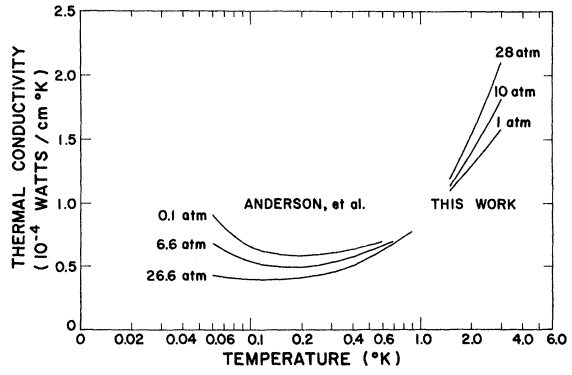

FIG. 7. Coefficient of thermal conductivity of liquid He^3 as a function of temperature for various pressures, showing the inversion of the pressure dependence near 1°K (low temperature curves drawn after Anderson *et al.*[14]).

been observed – and in this connection we note that Eq. (13) with constants of Table III should not be used for extrapolation below 1.5°K.

C. Liquid He^4 I Near the λ Transition

Some detailed data for the pressure dependence of κ of He^4 I in the region near the λ line are shown in Fig. 8. Those isotherms which intersect the λ line (i.e., $T < T_\lambda \sim 2.17$°K) behave at high pressures similarly to isotherms above 2.17°K; but as the λ line is approached from higher pressures, κ along an isotherm passes through a broad, shallow minimum and then rises steeply close to $T_\lambda(P)$. Because of the shape of the dips, the exact pressures of the minima are difficult to fix; in spite of these uncertainties, as graphed in Fig. 9, the location of these minima on the P-T plane appear to lie along a curve uniformly displaced from the λ line by about 0.030-0.040°K. It is unlikely that the rise in κ is directly associated with the P-T locus of $\alpha_P = 0$, signaling the anomalous behavior of α_P (also drawn in Fig. 9). These features near the λ line are related to the behavior of κ away from the transition in Fig. 10, where the κ-T-P surface and its projections are schematically represented. The surface was constructed from information such as shown in Figs. 6 and 8.

Recently, moderate success has been achieved in treating experimentally determined static critical-point properties by the so-called "scaling laws".[16,17] Rather than laws, these are hypotheses about the symmetry of second-order phase transitions which lead to a formulation of the limiting behavior of singular thermodynamic properties in terms of $|T-T_c|^n$. Here T_c is the critical temperature of the phase transition and n is an exponent characteristic of the property; the theory gives various relations between the exponents so as to restrict the number of independent exponents to two, even though the number of singular properties at T_c may be much larger than this. At the heart of this reasoning is the supposition that *near* T_c correlation lengths for the system become larger than the interatomic spacing; but *at* T_c the only relevant length for the system is the interatomic spacing, since all correlation lengths become infinite at T_c. Consequently the nature of the forces responsible for the transition are immaterial, so that all second-order phase transitions, including liquid-vapor critical points and λ transitions, should be, according to this hypothesis, fundamentally similar.

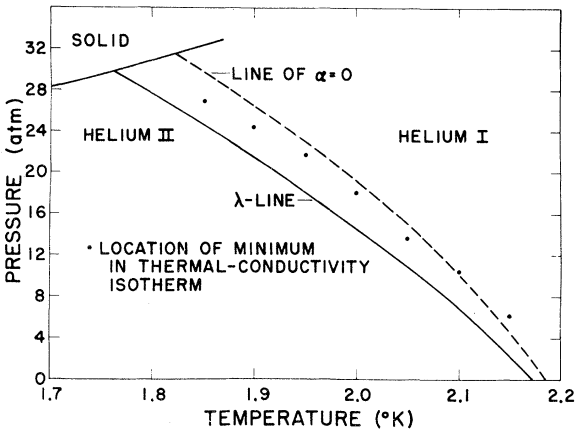

FIG. 9. P-T phase diagram of He^4 showing the relation among the locus of thermal-conductivity minima, the $\alpha_P = 0$ locus, and the λ line.

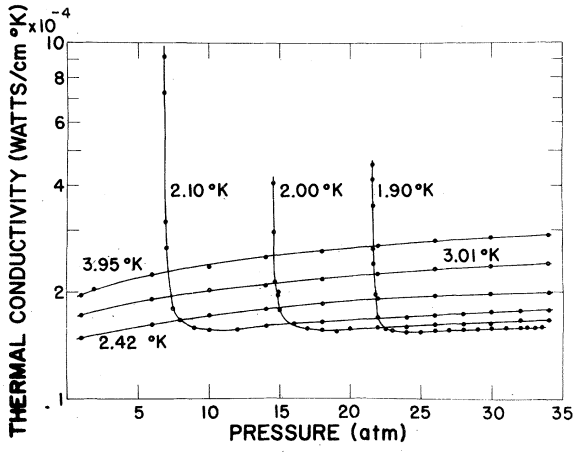

FIG. 8. Coefficient of thermal conductivity of liquid He^4 as a function of pressure at several temperatures, comparing the behavior of isotherms which intersect the λ line ($T < 2.17$° K) with those which do not ($T > 2.17$° K).

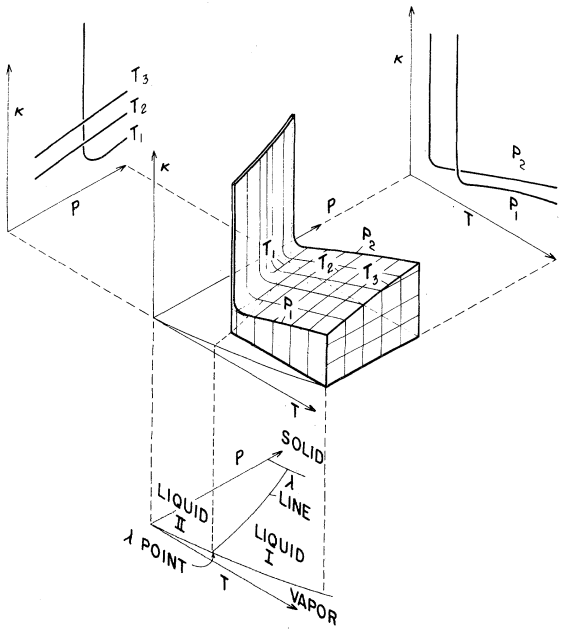

FIG. 10. Schematic plot of the κ-T-P surface and its projections for He^4I.

Several authors[18–20] have extended the scaling-law arguments to include dynamic properties near thermodynamic singular points. In particular, Ferrell *et al.*[18] have examined the fluctuations associated with first sound in He I and second sound in He II, both as $|t_\lambda| \equiv |T - T_\lambda| \to 0$. The result of this work is to suggest the temperature behavior for the damping of the sound modes near T_λ, which the authors in turn relate to the thermal conductivity on the high-temperature side of T_λ. They find

$$\kappa = \kappa_0 \left(\frac{2T_\lambda}{t_\lambda}\right)^{1/3} \ln^{1/2}\left(\frac{2T_\lambda}{t_\lambda}\right) \tag{14}$$

with $\kappa_0 = 1.36 \times 10^{-5}$ W/cm °K. The principal temperature dependence of κ resides in the term $(2T_\lambda/t_\lambda)^{1/3}$.

Equation (14) predicts the temperature variation of κ, whereas the results reported here represent $\kappa(P)$ along isotherms at several values of T_0. However, each point on an isotherm (at fixed T_0 and P) was obtained from a series of Q-ΔT measurements, which may be related to the temperature variation of κ through Eq. (4). Ferrell *et al.* have analyzed the present data in terms of Eq. (14) using the Q versus ΔT measurements for T_0 closest to T_λ at several pressures. Figures 9 and 10 of their paper show the agreement between theory and experiment to be good when κ_0 is normalized to the data (although the calculated value of κ_0 is about one-third too low, the authors consider this satisfactory considering the approximations made in the theory). They have also compared the data with Eq. (14) omitting the logarithmic factor and find fits very nearly as good.

On the other hand, if one assumes that near the λ line $\kappa(T)$ should be of the form

$$\kappa(T) = \alpha(T - T_\lambda)^{-\beta} = \alpha(1/t_\lambda)^{\beta}, \tag{15}$$

integration of Eq. (4) gives

$$Q(T_0, \Delta T) = (A/l)[\alpha/(1-\beta)] \times [T_0 + \Delta T - T_\lambda)^{1-\beta} - (T_0 - T_\lambda)^{1-\beta}], \tag{16}$$

and one may use the measurements to obtain α and β by a least-squares method. The results of such an analysis indicate: (1) There is no systematic variation of α and β along $T_\lambda(P)$, but if α increases, the corresponding β decreases. (2) Values of β range from 0.266 to 0.795, with all but one value greater than $\frac{1}{3}$. (3) If it is assumed that β should have a single value along $T_\lambda(P)$, a properly weighted average yields $\beta = 0.490$, significantly larger than the scaling-law predictions.

We have made a similar analysis using an equation of the form of Eq. (14) and calling the variable exponent β'. The conclusions are qualitatively the same as given in the preceding paragraph, except that the average value of β' is 0.423, still significantly different from the $\beta' = \frac{1}{3}$ of Ferrell *et al.*[18]

In all of these treatments a difficulty arises in assigning P-T coordinates to the λ line, and it is clear that the results obtained from using relations such as Eq. (16) depend sensitively upon the choice of T_λ. In the present work, (P_λ, T_λ) points were determined by the disappearance of ΔT when a constant, small, heat flow ($Q = 1.6 \times 10^{-5}$ W) was applied across the He⁴ sample, and the cell pressure was slowly lowered isothermally through the transition; the reappearance of ΔT on raising the pressure was also observed. For a given T the measurements in the two directions differed by no more than ± 0.005 atm. Parameters for the λ line so obtained agree well with other recent measurements,[21,22] especially those of Kierstead,[21] as shown in the abbreviated listing of Table IV. Even so, we have no real assurance that these are known with sufficient accuracy to allow a proper determination of β or β'. For each isotherm we require in Eqs. (14) and (15) values of T_λ corresponding to the pressures of the sample fluid. These were calculated from our measurements of P_λ and the slope of the λ line at the isotherm temperatures T_0. Thus we have

$$T_0 - T_\lambda = (P_\lambda - P)(dP/dT)_\lambda^{-1}. \tag{17}$$

Our conclusions are that while Eq. (14) is compatible with the experimental results, the best value of the exponent β' derivable from the data is not $\frac{1}{3}$ but 0.423.

D. Fluid He³ Near the Critical Point

The He³ 1962 scale of temperatures[23] gives for He³ $T_c = 3.324 \pm 0.0018$°K, $P_c = 1.149 \pm 0.002$ atm. Recently Zimmerman and Chase[24] have seriously challenged this value of T_c and concluded from their orthobaric density determinations that T_c should be 3.3088°K. If we give preference to the latter value of T_c and correct for the amount of He⁴ present in our He³ sample, we estimate $T_c = 3.317$°K for the experiments under discussion.

Figure 11 shows an over-all plot of κ for He³ as a function of pressure, while Fig. 12 gives details of the data for five isotherms in the critical region. According to the above, only the isotherm at 3.310°K lies below T_c. All of the isotherms have pronounced peaks even well above T_c, and in fact an isotherm at 3.95°K still exhibits remnants of

TABLE IV. Temperature-pressure coordinates of the λ line.

	λ pressure (atm)		
Temperature	This work	Kierstead[21]	Elwell and Meyer[22]
1.7701	29.36	29.37	29.33
1.8009	27.62	27.62	27.57
1.8995	21.59	21.58	21.54
1.9510	18.15	18.15	18.13
2.0020	14.54	14.54	14.54
2.0511	10.82	10.82	10.85
2.1000	6.852	6.84	6.89
2.1447	2.869	2.84	2.92
2.1501	2.335	2.32	2.40

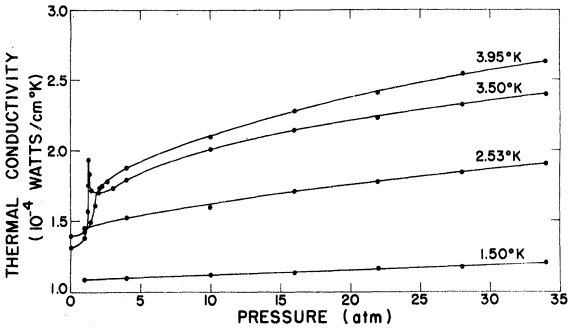

FIG. 11. Isotherms of thermal-conductivity coefficient versus pressure for He^3.

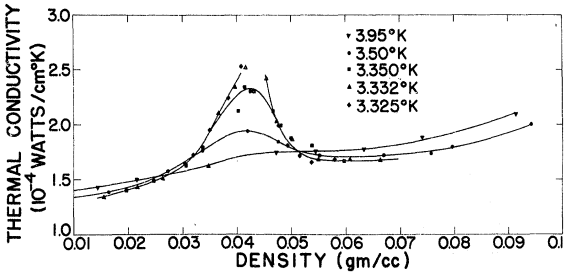

FIG. 13. Isotherms of thermal-conductivity coefficient versus density for He^3 near its critical point.

the critical-region behavior. Steady-state conditions were difficult to achieve on the steeply rising portions of isotherms between 3.325 and 3.350°K; for the highest conductivities measured here the estimated error is ±5% and no claim can be made for the determination of the height of the maxima. However, for isotherms above 3.350°K the maxima are clearly defined. A plot of the P-T locus of these maxima forms a smooth extension beyond the critical point of the saturated vapor pressure of the liquid (assuming $\ln P_{\text{sat}}$ is linear in $1/T$).

A more fundamental way of plotting the data is to consider κ a function of T and density ρ. Such a description is shown in Fig. 13, where the density values for various isotherms have been calculated from a modified Strobridge equation of state. This latter relation has the form

$$P = E_1\rho + E_2\rho^2 + E_3\rho^3 + E_4\rho^4 + E_5\rho^6 + (E_6\rho^3 + E_7\rho^5)\exp(-E_8\rho^2) \quad (18)$$

with E_i a function of T only. The E_i have been evaluated by Kerr and Sherman.[25] Near the critical density, $\rho_c = 0.042$ g/cm³, the relation is based on a very limited amount of data. Since here ρ is a very strong function of P and T, the isotherms at 3.325, 3.332, and 3.350°K shown in Fig. 13 must be considered approximate. Nevertheless, this plot has the advantages over the pressure representation of spreading out the critical region and of showing more directly the growth of the peaks in κ as $T \to T_c$.

We also point out that Fig. 5 illustrates for the 1-atm isobar how κ behaves at the liquid-vapor transition just below the critical point. Data such as shown in Figs. 5 and 11 have been combined to construct the schematic κ-T-P surface of Fig. 14 which emphasizes the anomalies near T_c.

Although a fully developed theory for transport phenomena in the critical region does not exist, the behavior of κ has been a subject of recent interest. Fixman[26] and Mountain and Zwanzig[27] have predicted that κ should diverge along the critical isochore as $(T - T_c)^{-1/2} \equiv t_c^{-1/2}$, whereas Kadanoff and Swift[20] indicate the singularity should proceed as $t_c^{-2/3}$. The latter result comes from a scaling-law argument applied to a classical liquid; but the authors estimated that the critical exponent should not be materially altered because of the presence of quantum effects. Unfortunately, the scatter in the present data precludes a definitive analysis for making a choice between these (or any other strongly singular) limiting forms.

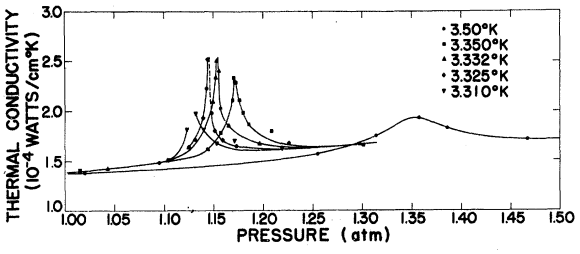

FIG. 12. Isotherms of thermal-conductivity coefficient versus pressure for He^3 near its critical point.

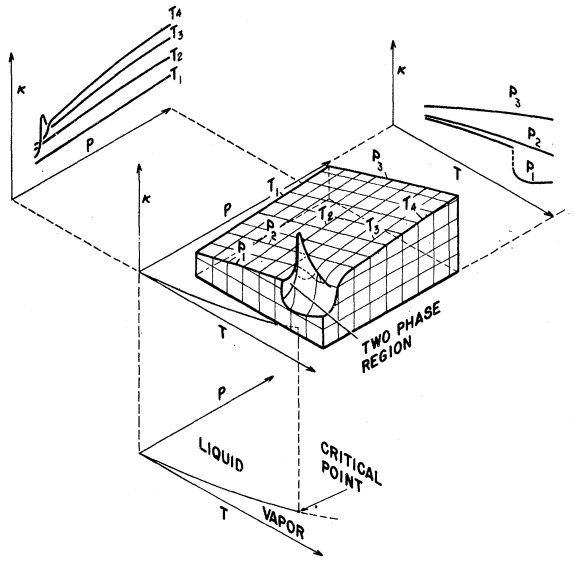

FIG. 14. Schematic plot of the κ-T-P surface and its projections for fluid He^3.

V. CONCLUSIONS

While within the stated limits of accuracy we have no reservations about the quality of the data presented here, they are clearly not sufficiently precise to give answers about some important questions regarding the thermal conductivity of the helium isotopes. In regions well away from anomalies associated with thermodynamic singularities these studies give well-defined results such that we have no hesitation in handing them to the theorist with a request for an explanation. But near the λ point of He^4 and the critical point of He^3 the experiments show only the qualitative behavior predicted by theory. The demand for precision is much higher here, and one can only guess at how many orders-of-magnitude more precise the data must be to confirm or refute the several proposals for the limiting forms of $\kappa(T, P)$ as $T \to T_\lambda$ or as $T \to T_c$.[28] We must realize, of course, that experimentally it is impossible to observe an infinite thermal conductivity, so that the theoretical divergences can be tested only as the singular points are closely approached. Perhaps even more delicate is the question of how (or if) quantum effects enter the picture at T_c, since as yet no gross features have emerged to indicate this. To compare the critical singularities of helium with classical fluids we require much better information than we have now on both classes of substances.

ACKNOWLEDGMENTS

We are especially grateful to Dr. L. Goldstein, Dr. E. F. Hammel, and Dr. D. McLaughlin for their continued interest and helpful discussions during the course of this work, to Dr. R. Moore and Dr. R. H. Sherman for their aid in several computing problems, and to G. Bjarke for his assistance with electrical standards equipment.

---

*Work done under the auspices of the U. S. Atomic Energy Commission.

†Based in part on a Ph.D. thesis by Jerry F. Kerrisk, the University of New Mexico, 1968.

[1]C. Grenier, Phys. Rev. 83, 598 (1951).

[2]R. Bowers, Proc. Phys. Soc. (London) A65, 511 (1952).

[3]L. J. Challis and J. Wilks, in Proceedings of the Symposium on Solid and Liquid He^3, U. S. Air Force Office of Scientific Research Report No. TR-57-78 (Ohio State University Research Institute, Columbus, Ohio, 1957), p. 38.

[4]D. M. Lee and H. A. Fairbank, Phys. Rev. 116, 1359 (1959).

[5]F. G. Brickwedde, H. van Dijk, M. Durieux, J. R. Clement, and J. K. Logan, The "1958 He^4 Scale of Temperatures", Natl. Bur. Std. Monograph 10, (U. S. Government Printing Office, Washington, D. C., 1960).

[6]G. O. Bjarke, in Proceedings of the International Institute of Refrigeration, Liquid Helium Technology, Comm. I, Boulder, Colorado (Pergamon Press, London, 1966).

[7]H. S. Sommers, Jr., Rev. Sci. Inst. 25, 793 (1954).

[8]R. B. Lazarus, Rev. Sci. Inst. 34, 1218 (1963).

[9]W. E. Deming, Statistical Adjustment of Data (John Wiley & Sons, Inc., New York, 1943).

[10]A. Michels and J. V. Sengers, Physica 28, 1238 (1962).

[11]I. Catton, Phys. Fluids 9. 2512 (1966).

[12]F. Fokkens, W. Vermeer, K. W. Taconis, and R. De Bruyn Ouboter, Physica 30, 2153 (1964).

[13]J. F. Kerrisk, Ph.D. thesis, University of New Mexico, 1968 (unpublished).

[14]A. C. Anderson, J. I. Connolly, O. E. Vilches, and J. C. Wheatley, Phys. Rev. 147, 86 (1966).

[15]A. A. Abrikosov and I. M. Khalatnikov, Rep. Progr. Phys. 22, 329 (1959).

[16]B. Widom, J. Chem. Phys. 43, 3892, 3898 (1965).

[17]L. P. Kadanoff, Physics 2, 263 (1966).

[18]R. A. Ferrell, M. Menyhard, H. Schmidt, F. Schwabl, and P. Szepfalusy, Phys. Rev. Letters 18, 891 (1967); Ann. Phys. (N. Y.) 47, 565 (1968).

[19]B. I. Halperin and P. C. Hohenberg, Phys. Rev. Letters 19, 700 (1967).

[20]L. P. Kadanoff and J. Swift, Phys. Rev. 166, 89 (1968).

[21]H. A. Kierstead, Phys. Rev. 162, 153 (1967).

[22]D. L. Elwell and H. Meyer, Phys. Rev. 164, 245 (1967).

[23]S. G. Sydoriak and R. H. Sherman, J. Res. Natl. Bur. Std. A68, 547 (1964).

[24]G. O. Zimmerman and C. E. Chase, Phys. Rev. Letters 19, 151 (1967).

[25]E. C. Kerr and R. H. Sherman, Proceedings of the Tenth International Conference on Low Temperature Physics, edited by M. P. Malkov (Viniti, Moscow, 1967), Vol. 1, p. 325.

[26]M. Fixman, J. Chem. Phys. 47, 2808 (1967).

[27]R. D. Mountain and R. Zwanzig, J. Chem. Phys. 48, 1451 (1968).

[28]*Added in proof.* G. Ahlers [Phys. Rev. Letters 21, 1159 (1968)] has recently shown that in He I, $\kappa \propto t_\lambda^{-\beta}$ with $\beta = 0.334 \pm 0.005$ for $10^{-7} \leq t_\lambda \leq 5 \times 10^{-4}$ °K.